Hindawi
Journal of Spectroscopy
Volume 2018, Article ID 4893274, 8 pages
https://doi.org/10.1155/2018/4893274

Research Article

Surface-Enhanced Raman Spectroscopy Analysis of Human Breast Cancer via Silver Nanoparticles: An Examination of Fabrication Methods

Beata Brozek-Pluska, Monika Kopec, and Jakub Surmacki

Laboratory of Laser Molecular Spectroscopy, Institute of Applied Radiation Chemistry, Lodz University of Technology, Lodz, Poland

Correspondence should be addressed to Beata Brozek-Pluska; beata.brozek-pluska@p.lodz.pl

Received 18 December 2017; Revised 27 March 2018; Accepted 31 May 2018; Published 15 July 2018

Academic Editor: Feride Severcan

Copyright © 2018 Beata Brozek-Pluska et al. This is an open access article distributed under the Creative Commons Attribution License, which permits unrestricted use, distribution, and reproduction in any medium, provided the original work is properly cited.

Breast cancer in a traditional way is diagnosed using mammography, computer tomography, ultrasounds, biopsy, and finally, histopathological analysis. Histopathological analysis is a gold standard in breast cancer diagnostics; however, it is time consuming and prone to the human interpretations. That is why new methods based on optical properties of analyzed human tissue samples are needed to be introduced to the clinical practice objective, costless and fast diagnostic protocols. Nowadays, Raman spectroscopy-based methods are gaining more and more importance. Raman spectroscopy and imaging allow to characterize human tissue samples using an electromagnetic radiation from a safe range, and simultaneously, a minimal sample preparation is required. During measurements, a natural differentiation in tissues components' scattering cross sections is used to build 2D and 3D maps of the chemical component distribution. The paper presents the application of SERS (surface-enhanced Raman spectroscopy) measurements for analysis of human breast cancer (adenocarcinoma). The advantages of SERS application in cancer diagnostics are also discussed. Moreover, the detailed chemical composition of human breast cancer tissue based on Raman bands of DNA/RNA, amino acids, lipids, and proteins which are significantly enhanced is presented. Three different methods of NP preparation are presented, and the effectiveness of Raman signal enhancement of Ag nanoparticles synthetized by these methods is compared. The enhancement effect of NPs synthetized by reduction of silver nitrate with sodium borohydride (method no. 1) and silver nitrate-hydroxylamine hydrochloride reduction (method no. 2) was stronger when compared with the polyol method (method no. 3). Presented SERS results confirmed that the clearly resolved and high-intensity Raman spectra of cancer human breast tissue can be recorded using integration times of the order of fractional seconds and one milliwatt of the excitation laser power.

1. Introduction

In the twenty-first century, cancer, just after cardiovascular diseases, is one of the leading causes of deaths in people around the world. The magnitude of this problem concerns both the epidemiological and diagnostic aspect. In 2017, 1,688,780 new cancer cases and 600,920 cancer deaths were projected to occur in the United States [1]. Such a statistic confirms that cancer is a global problem and remains an unsolved challenge. Various techniques such as MRI, mammography, ultrasonography, and positron emission tomography (PET) are used for detection of pathological cells at different stages of cancer development.

MRI screening is characterized by significantly higher sensitivity than typical for mammography (92.3% versus 30.8%), but simultaneously lower specificity for MRI is noticed (85.9% versus 96.8%) [2]. Even if the sensitivity and the specificity for the abovementioned methods can reach more than 90%, strong magnetic field or X-ray radiation constitutes undisputed disadvantages. Ultrasonography is completely safe for patients but has a low sensitivity equal to around 71.1% among women with predominantly fatty breast and only 57.0% for heterogeneous dense breasts, and the specificity for this technique is estimated around 88.5% [3]. The ability of PET to detect breast cancer strongly depends on the tumor's size, which should be considered as

a serious disadvantage. The sensitivity of PET has been reported to be 68% for small (<2 cm) tumors and 92% for larger (2–5 cm) ones; moreover, the accuracy for detecting carcinomas in situ is very low and equal to 2–25% [4].

However, the final outcome for cancer every time is defined by the pathological study of a biological material taken during the biopsy or surgery. Such material is used for preparation of standard histologically stained specimens. Unfortunately, the histopathological diagnostic methods are highly invasive and costly to the health-care system. Moreover, for mass screening patients, the histopathological diagnostic methods are time consuming and strongly prone to the human interpretations. That is why the need to introduce new methods, safe for patients, fast, and objective to reduce the number of biopsies and medical costs, as well as the need for the determination of many cancer markers simultaneously in one measurement is a motivation for many researchers to introduce spectroscopic techniques in diagnostics of cancer [5–14].

Spectroscopic techniques based on Raman scattering have been proven to be powerful diagnostic tools providing objective biochemical fingerprints to distinguish normal, benign, and cancer tissues of many organs: lungs [5] based on nuclei acids and phospholipids; breast [6–13] based on proteins, lipids, and water; esophageal [14] based on DNA/RNA, proteins, and collagen contents; and gastric based on the relative amounts of nucleic acid, collagen, phospholipids, phenylalanine, and saccharide [15].

The key advantages of Raman spectroscopy (RS) over the traditional diagnostics methods are as follows: the capability of providing objective biochemical information about the components of normal, benign, and cancer cells and possibility to identify different cancer markers in one measurement. Advantages of RS over other spectroscopic techniques such as IR spectroscopy, for example, are a lack of interference from water, which is particularly important for live-cell, human tissue analysis and in vivo applications. RS offers also high spatial resolution [7–13]. The main disadvantage of Raman-based optical methods is that even if Raman spectra are really informative and accurate, the Raman signal is very weak, which can limit its applications for diagnosis of early stages of cancer samples.

Therefore, there is a really need to develop new procedures to generate a simple approach that ensures high-quality spectrum. Surface-enhanced Raman spectroscopy (SERS) opens new possibilities to overcome the limitations of conventional RS. SERS enables much better limits of detection enabling single-molecule detection level. Simultaneously, there are many variables that need to be optimized to obtain the enhanced Raman signal of the analyzed biological sample.

SERS is based on the excited surface plasmons in a rough metallic surface. The amplification factors typical for the Raman signal in SERS technique are equal to 10^6–10^8 [16]; that is why in the fingerprint region of recorded vibrational spectra, intense and sharp bands can be observed [17–19]. This makes SERS a great multiplexing technique characterizing by very high sensitivity even in the picomolar range [20].

Metals that are used in SERS techniques are Ag, Au, and Cu. Nanoparticles (NPs) of these metals are characterized by intense absorption bands in the UV-Vis region, which are not present in the spectrum of the bulk metal.

The strongest enhancement in SERS is observed when the frequency of incident photon is in resonance with the oscillation of conduction electrons; that is why the excitation wavelength in SERS experiments must be coupled with absorption properties of synthetized NPs.

Recent SERS technique was successfully applied in molecular diagnosis, in vivo imaging, and drug delivery using nanoparticles such as nanocrystals, quantum dots, biodegradable nanoparticles, and nanoscale carriers [21–24]. Metal NPs functionalized with sensitive Raman reporter molecules followed by bioconjugation have been applied for labeling biological systems in cells and tissues as a noninvasive imaging technique with picomolar sensitivity and multiplexing capabilities [25, 26]. Chemical inactivity of Au and Ag nanoparticles also makes them most suitable for introduction into living cells as SERS nanoprobes to enhance the Raman signal.

In our previous work, we found that spontaneous Raman scattering technique can be applied to distinguish cancerous from noncancerous human breast tissues [7–13].

In this paper, we applied the SERS technique for analysis of nonfixed human breast cancer slices using Ag colloidal nanoparticles. Presented results confirmed that the SERS technique is a powerful tool with high sensitivity for screening of chemical compounds in a sample, being of great importance for the purposes of biomedical research especially the early diagnosis of any cancer. The comparison of physical properties of nanoparticles synthetized using different methods and the comparison of efficiency of signal enhancement will also be discussed.

2. Experimental Methods

2.1. Tissue Samples. We examined cryosectioned slides (6 μm thin) of adenocarcinoma (results for one patient number, P141, from a database of 250 patients, are presented). We recorded 100 spectra for each sample. The research did not affect the course of the operation or treatment of the patients. The tissue was obtained during a surgical operation, cut into thin sections at −25°C, and mounted on CaF_2 windows. For SERS measurements, tissue slices were covered by 4-5 drops (~200–250 μL) of nanoparticle solutions per each sample. Dried samples were analyzed immediately. All procedures have been conducted under a protocol approved by the Bioethical Committee at the Medical University of Lodz (RNN/323/17/KE/17/10/2017).

2.2. Raman Microspectroscopy. Raman spectra were acquired with a confocal Alpha 300RSA+ Raman microscope (WITec) operating at 532 nm laser excitation with an ultrahigh-throughput spectrometer, an Andor Newton DU970N-UVB-353 CCD Camera, and a 40x dry objective (Nikon, CFI Plan Fluor C ELWD DIC-M, NA of 0.60, and a 3.6–2.8 mm WD). A single SERS spectrum was recorded with an integration time of 0.1 second at 532 nm excitation (average laser power: 1 mW). WITec Project Plus (WITec

GmbH, Germany) and Origin (OriginLab) were used for data acquisition and analysis, respectively.

2.3. Nanoparticle Synthesis

2.3.1. Method No. 1. We have mixed 2.0 mL of 1.25×10^{-2} M sodium citrate, 5.0 mL of 3.75×10^{-4} M silver nitrate, and 5.0 mL of 5.0×10^{-2} M hydrogen peroxide. Then, a 20 mL of 1.0×10^{-3} M potassium bromide was added. For the final silver reduction step, 2.5 mL of freshly prepared 5.0×10^{-3} M sodium borohydride was mixed with the solution. Excess sodium citrate was used as a buffer to preserve neutral or weakly basic pH of the solution to stabilize the synthetized silver nanoprisms. Hydrogen peroxide was employed to facilitate formation of shape-selected particles. In the absence of peroxide, uncontrolled growth of NPs with a large number of structural defects can be observed [27]. Finally, the silver NPs were analyzed with a high-resolution scanning electron microscope.

2.3.2. Method No. 2. We have mixed the silver nitrate in the concentration of 10^{-3} M with hydroxylamine hydrochloride in the concentration of 1.5×10^{-3} M. Hydroxylamine hydrochloride was preserved at an initial alkaline pH of the reaction. The final pH of the colloidal solution was optimized by varying the amount of sodium hydroxide added to the hydroxylamine solution, and pH of 7 for the reduction reaction during the experiment was kept. The reaction was completed within a few seconds [28]. Finally, the silver NPs were analyzed with a high-resolution scanning electron microscope.

2.3.3. Method No. 3. Silica NPs were prepared using ammonium hydroxide, dry ethanol, and tetraethyl orthosilicate (TEOS) by stirring mixture for 24 h at 25°C. The formed silica NPs were purified and functionalized with 3-mercaptopropyltrimethoxysilane (MPTS). The polyol method [29] was used for the preparation of silver nanoparticle-embedded silica spheres. Finally, the NPs were analyzed with a high-resolution scanning electron microscope.

2.4. SEM, UV-Vis, and DLS Measurements. The UV-Vis spectroscopy, SEM, and DLS measurements were performed to characterize the size and morphology of the produced colloids. UV-Vis spectra were recorded with a Varian Cary 5E spectrophotometer and 2 mm quartz cells (Hellma). DLS measurements were performed using Zetasizer Nano Z. SEM measurements were obtained using a microscope SEM S-4700 Hitachi.

3. Results and Discussion

In this section, the results of the confocal Raman microspectroscopy for the cancerous human breast tissues of the patient P141 (patient no. 141 from a database of 250 patients) before and after addition of nanoparticles are presented. The typical results for the patient P141 have been used to illustrate the most important findings of research.

In our previous paper, we have proved that Raman spectroscopy can be successfully implemented to discriminate between noncancerous and cancerous breast tissues [7–13]; that is why in this section, we have focused only on the cancerous tissue analysis to show that using SERS one can identify a single pathology cells.

Before we start the analysis of biological SERS spectra, the characterization of NPs synthetized by different methods is needed.

Historically, metallic electrodes were first used as active enhanced supports, and then, metallic NPs in solutions and finally metallic nanostructures like arrays on a flat substrate were used to improve the sensitivity of RS over last 10 years [30].

NP solutions have several advantages compared to the other enhanced supports including ease of colloid formation and straightforward characterization of the colloid solution by simple UV-Vis absorption measurements. On the other hand, the size of NPs in colloidal solutions cannot be uniform, and not negligible problems can be observed due to instability of such a system [31, 32].

Figure 1 presents UV-Vis spectra and SEM images of all three types of NP colloidal solutions used in SERS human breast tissue measurements.

One can see from Figure 1 that the maximum peak position for the absorbance for all NPs is observed in the spectral range 440–485 nm, but not negligible absorbance, compared to the maximum value of 532 nm, used in our experiments as an excitation laser wavelength, is also observed. This observation confirms that the 532 nm wavelength is suitable for the plasmon generation of Ag nanoparticles.

Simultaneously, the comparison for NPs synthetized in our group using different methods shows that the highest value of the absorbance is noticed for the NPs produced by method no. 1 where borohydride was used as a reduction agent.

The colloids characterized by UV-Vis spectra were also analyzed using SEM technique. Figures 1(b), 1(d), and 1(f) show SEM images of colloidal solutions of NPs prepared to test in SERS measurements of human cancer breast tissues.

The characteristic of NP morphology was completed by DLS measurements. Table 1 presents information about the size of NPs prepared by different methods.

The differences between the results obtained using SEM technique and DLS measurements can be explained by the fact that the aggregation of NPs during DLS and SEM measurements is observed.

The SERS activity of synthetized colloids was tested using human cancerous tissues of the same patient P141. Figure 2 presents the SERS spectra of human cancer slices (laser power 1 mW, integration time 0.1 sec) recorded using synthetized NP colloids and the native Raman spectra recorded for the same tissue sample.

One can see that Figures 2(a)–2(f) show the clearly resolved and high-intensity SERS spectra of cancerous human breast tissue with added Ag solutions. The regular

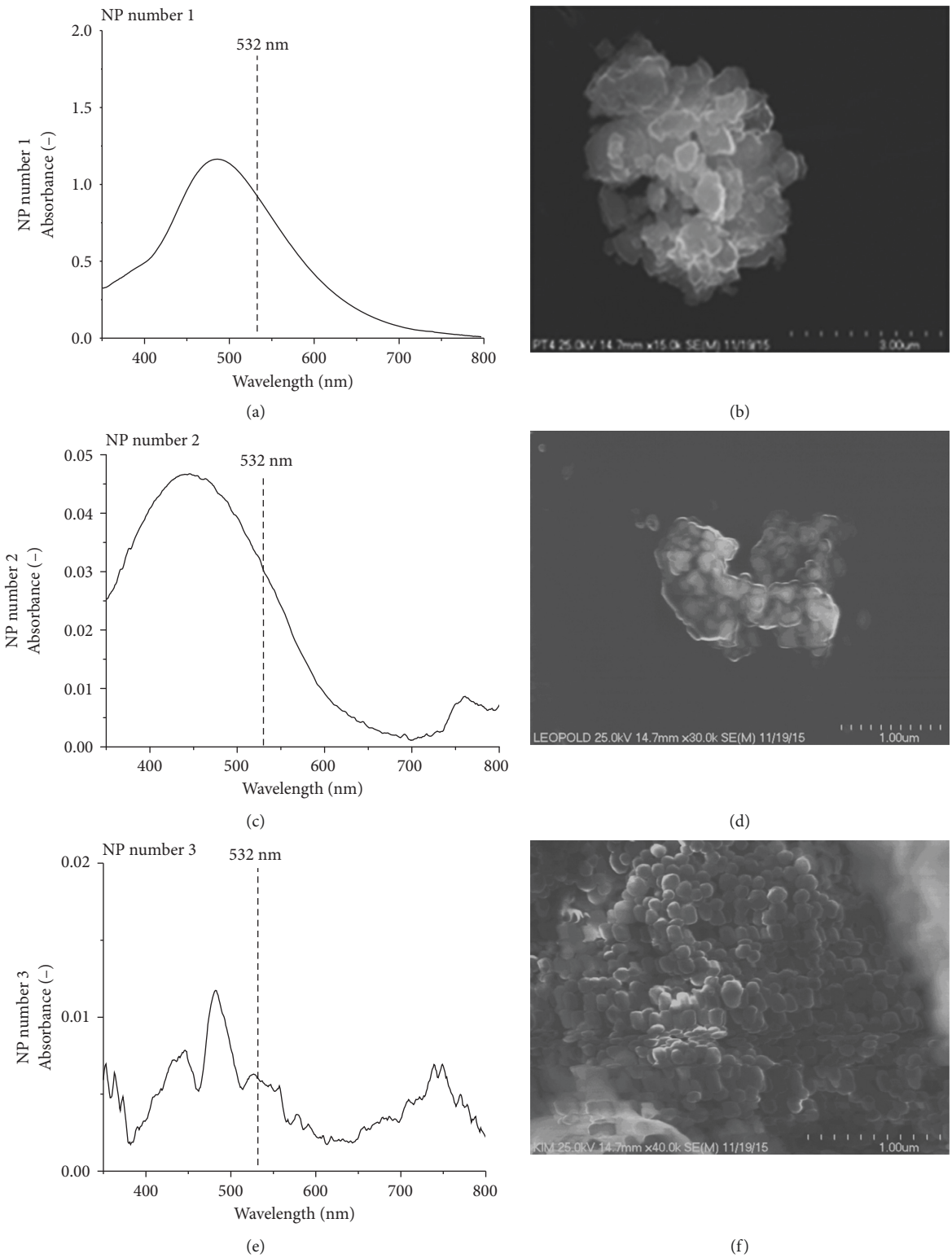

Figure 1: UV-Vis spectra (a, c, e) and SEM images (b, d, f) of NPs synthetized by different methods described in detail in the experimental section.

Raman spectrum of the cancerous sample without Ag sol is shown in Figure 2(g). In the native tissue sample without the addition of silver colloid solution for the integration time of 0.1 sec. and the laser power of 1 mW, no Raman peaks were observed. A comparison of data presented in Figures 2(a)–2(g) clearly demonstrates that Ag colloid enhanced dramatically

Table 1: The average size of NPs determined using the DLS method.

Method	The average size of NPs determined using the DLS method
No. 1	64 nm
No. 2	118 nm
No. 3	296 nm

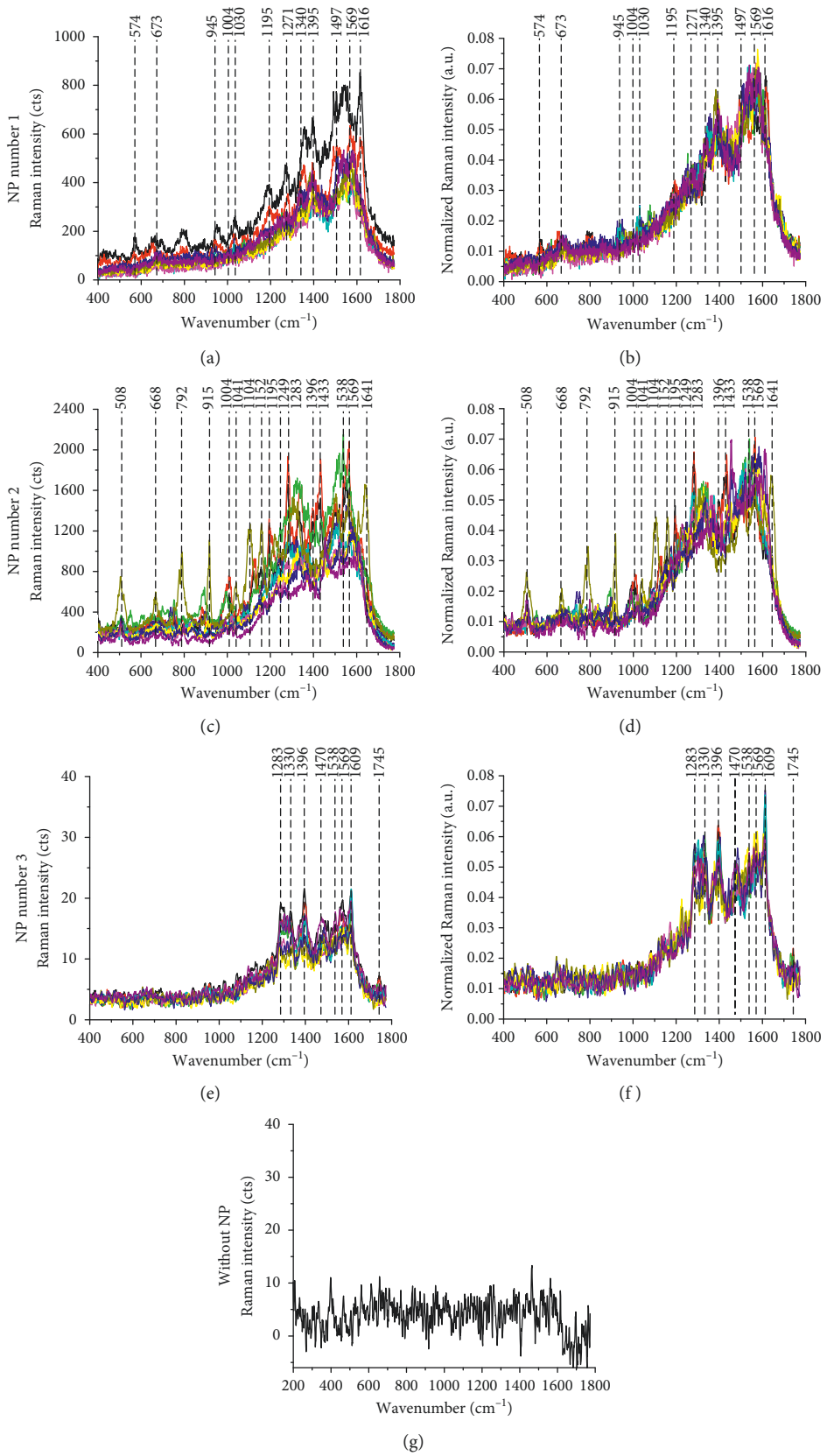

FIGURE 2: Raw (a, c, e) and vector-normalized (b, d, f) SERS spectra of human cancerous breast tissue of the patient P141 and the native Raman spectra (g) recorded for the same tissue sample; excitation wavelength: 532 nm, integration time 0.1 sec, and laser power 1 mW.

Table 2: Maximum peak positions of Raman bands observed for SERS spectra and the tentative assignments of these bands.

Maximum peak position in SERS spectrum (cm^{-1})	Tentative assignment [36]
547	Cholesterol
668, 673	C–S stretching mode of cysteine, T, G (DNA/RNA), C–S stretching mode of cytosine
945	Valine, proline, and polysaccharides
1004	Phenylalanine
1030	Phenylalanine of collagen
1095	Symmetric PO_2^- stretching vibration of the DNA backbone; phosphate backbone vibration as a marker mode for the DNA concentration; C–N of proteins
1152	ν(C–N), proteins
1249	Thymine, adenine, DNA, RNA, phospholipids, Amide III, lipids, fatty acids
1271	Typical phospholipids, Amide III band in proteins, a C–N stretch from alpha helix proteins
1283	Lipids and fatty acids
1340	DNA, RNA
1395	Lipids and fatty acids
1497	Proteins and lipids
1569	Amides, vibrations of C=O, C–N, and N–H groups
1609	Cytosine (NH_2)
1745	ν(C=O), phospholipids, and triglycerides (lipid and fatty acids assignment)

the intensity of vibration bands that characterize the human cancer tissue, indicating that there is a strong interaction between the synthetized silver NPs and the analyzed tissue sample. The analysis of human breast tissue presented in Figures 2(a)–2(f) reveals that the significant SERS spectral signals typical for breast cancer structures are observed in a spectral range 500–1800 cm^{-1} and can be recorded for a split second. One can see from Figures 2(a)–2(f) that the main peaks observed for the tissue samples correspond to DNA/RNA, amino acids, lipids, and proteins. Our analysis confirms preliminary observation by González-Solís et al. [33], Guerrini et al. [34], Karabeber et al. [35], and our previous experiments using spontaneous Raman spectroscopy [7–13]. More detailed analysis of band intensity at ~1396 cm^{-1} observed in all SERS spectra of the three proposed methods shows that the mean ± SD are 527.1 ± 94.9, 906.5 ± 281.9, and 15.2 ± 3.3 for NP nos. 1, 2, and 3, respectively. The weak enhancement effect in the Raman observed in silver NP no. 3 by taking three different synthesis methods into consideration can be explained by smaller efficiency plasmon generation excited at $\lambda = 532$ nm (lower absorbance at 532 nm, see Figures 1(a), 1(c), and 1(e)).

Table 2 presents the maximum peak positions of Raman bands observed for SERS spectra and the tentative assignments of these bands based on [36].

For better comparison of the enhancement efficiency of synthetized NPs, all recorded SERS spectra were vector-normalized (Origin model: divided by Norm (length)).

One can see from Figures 2(b), 2(d), and 2(f) that the efficiency of Raman signal enhancement is comparable for NPs synthetized by the above-described different methods.

The efficiency of Raman signal enhancement for NPs synthetized by method no. 1, which is very simple in preparation compared to method nos. 2 and 3 and offers high Raman peak intensities for not normalized human breast cancerous tissue samples that can be commonly used for screening in medical measurements was also tested using the well-known Raman reporter compound 4-mercaptotoluene (4-MT). The objective of medical screening procedures is to detect cancerous cells in a very short time.

SERS measurements for this model compound, which can be finally used for functionalization of Ag NPs, confirmed that obtained silver nanostructures allow to record Raman spectra of 4-MT for picomolar concentrations. Figure 3 presents SERS spectrum of 4-mercaptotoluene for the concentration equal to 2.5×10^{-3} and 1.0×10^{-15} M (a) and the analysis of SERS Raman signal intensity in the function of 4-MT concentration (in a concentration range of 1.0×10^{-15}–2.5×10^{-3} M for peak recorded at 1079 cm^{-1}) (b).

One can see from Figure 3 that nonlinear correlation in the whole concentration range of 1.0×10^{-15}–2.5×10^{-3} M between SERS signal and the concentration of 4-MT is observed. The high linearity is observed for the concentration below 1×10^{-4} M and for the range 1×10^{-4}–2.5×10^{-3} M.

4. Conclusions

In this work, we have presented the biochemical characteristic of human breast cancer using SERS technique by recording fingerprint vibrations effectively enhanced by silver NPs. The application of NPs allowed to identify the biomolecules as amino acids (phenylalanine, tyrosine, and tryptophan), proteins, and DNA. We have shown that the SERS technique reduces exposure times to a split second for collecting good quality spectra with well-defined and isolated bands, whereas the conventional Raman spectroscopy requires at least one of several to hundred seconds for analysis. Our study confirmed that surface-enhanced Raman scattering maintains great possibilities to acquire hundreds

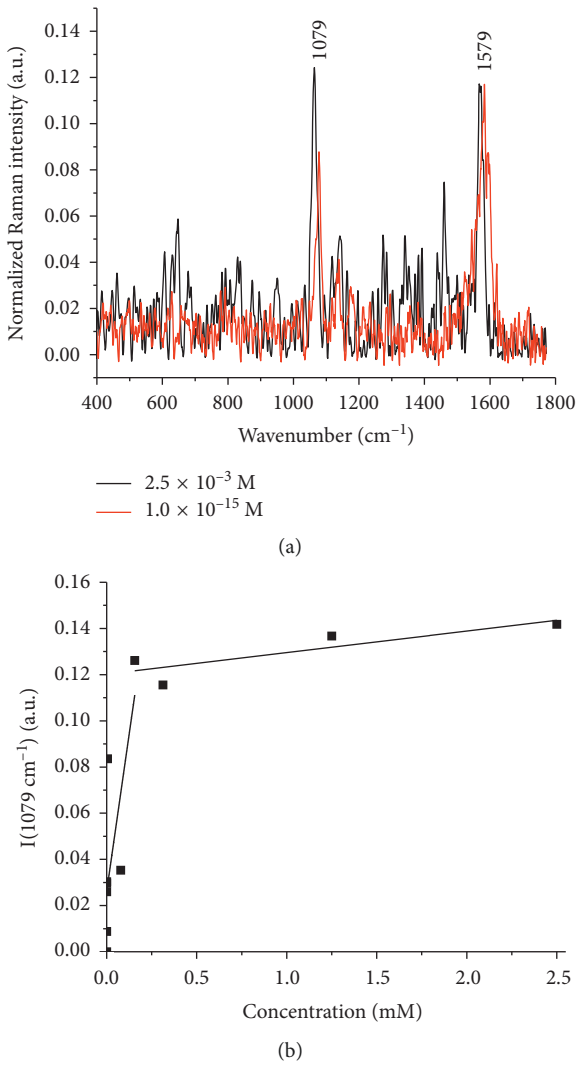

FIGURE 3: SERS spectrum of 4-mercaptotoluene (2.5×10^{-3} and 1.0×10^{-15} M) with NPs synthetized by method no. 1 (a). SERS Raman signal intensity in the function of 4-MT concentration in a concentration range of 1.0×10^{-15}–2.5×10^{-3} M (b).

of spectra of tissues in a very short time which is important for medical patient screening. Moreover, it is shown that the enhancement effect of NPs synthetized by simple reduction method is stronger in comparison with the polyol method. We have shown also that nonlinear correlation in the whole concentration range of 1.0×10^{-15}–2.5×10^{-3} M between SERS signal and the concentration of 4-MT is observed. The high linearity was observed for the concentration below 1×10^{-4} M and for the range 1×10^{-4}–2.5×10^{-3} M.

Conflicts of Interest

The authors declare that there are no conflicts of interest regarding the publication of this paper.

Acknowledgments

The project was funded through the National Science Centre Poland Grant UMO-2015/19/B/ST4/01878 and Dz. St. 2018.

References

[1] R. L. Sieqel, K. D. Miller, and A. Jemal, "Cancer statistics, 2017," *CA: A Cancer Journal for Clinicians*, vol. 67, no. 1, pp. 7–30, 2017.

[2] A. Raikhlin, B. Curpen, E. Warner, C. Betel, B. Wright, and R. Jong, "Breast MRI as an adjunct to mammography for breast cancer screening in high-risk patients: retrospective review," *American Journal of Roentgenology*, vol. 204, no. 4, pp. 889–897, 2015.

[3] E. Devolli-Disha, S. Manxhuka-Kerliu, H. Ymeri, and A. Kutllovci, "Comparative accuracy of mammography and ultrasound in women with breast symptoms according to age and breast density," *Bosnian Journal of Basic Medical Sciences*, vol. 9, no. 2, pp. 131–136, 2009.

[4] S. K. Yang, N. Cho, and W. K. Moon, "The role of PET/CT for evaluating breast cancer," *Korean Journal of Radiology*, vol. 8, no. 5, pp. 429–437, 2007.

[5] Z. Huang, A. McWilliams, H. Lui, D. I. McLean, S. Lam, and H. Zeng, "Near-infrared Raman spectroscopy for optical diagnosis of lung cancer," *International Journal of Cancer*, vol. 107, no. 6, pp. 1047–1052, 2003.

[6] A. S. Haka, K. E. Shafer-Peltier, M. Fitzmaurice, J. Crowe, R. R. Dasari, and M. S. Feld, "Diagnosing breast cancer by using Raman spectroscopy," *Proceedings of the National Academy of Sciences*, vol. 102, no. 35, pp. 12371–12376, 2005.

[7] H. Abramczyk and B. Brozek-Pluska, "New look inside human breast ducts with Raman imaging. Raman candidates as diagnostic markers for breast cancer prognosis: mammaglobin, palmitic acid and sphingomyelin," *Analytica Chimica Acta*, vol. 909, pp. 91–100, 2016.

[8] B. Brozek-Pluska, M. Kopec, J. Surmacki, and H. Abramczyk, "Raman microspectroscopy of the noncancerous and the cancerous human breast tissues. Identification and phase transitions of linoleic and oleic acids by Raman spectroscopy and Raman low-temperature studies," *Analyst*, vol. 140, no. 7, pp. 2134–2143, 2015.

[9] J. Surmacki, B. Brozek-Pluska, R. Kordek, and H. Abramczyk, "The lipid-reactive oxygen species phenotype of breast cancer. Raman spectroscopy and mapping, PCA and PLSDA for invasive ductal carcinoma and invasive lobular carcinoma. Molecular tumorigenic mechanisms beyond Warburg effect," *Analyst*, vol. 140, no. 7, pp. 2121–2133, 2015.

[10] B. Brozek-Pluska, M. Kopec, I. Niedzwiecka, and A. Morawiec-Sztandera, "Label-free determination of lipids composition and secondary proteins structure of human salivary noncancerous and cancerous tissues by Raman microspectroscopy," *Analyst*, vol. 140, no. 7, pp. 2107–2113, 2015.

[11] H. Abramczyk, B. Brozek-Pluska, J. Surmacki, J. Musial, and R. Kordek, "Oncologic photodynamic diagnosis and therapy: Confocal Raman/fluorescence imaging of metal phthalocyanines in human breast cancer tissue in vitro," *Analyst*, vol. 139, no. 21, pp. 5547–5559, 2014.

[12] H. Abramczyk, B. Brozek-Pluska, M. Krzesniak, M. Kopec, and A. Morawiec-Sztandera, "The cellular environment of cancerous human tissue. Interfacial and dangling water as a "hydration fingerprint"," *Spectrochimica Acta Part A: Molecular and Biomolecular Spectroscopy*, vol. 129, pp. 609–623, 2014.

[13] H. Abramczyk and B. Brozek-Pluska, "Raman imaging in biochemical and biomedical applications. Diagnosis and treatment of breast cancer," *Chemical Reviews*, vol. 113, no. 8, pp. 5766–5781, 2013.

[14] S. Feng, J. Lin, Z. Huang et al., "Esophageal cancer detection based on tissue surface-enhanced Raman spectroscopy and

multivariate analysis," *Applied Physics Letters*, vol. 102, pp. 1–5, 2013.

[15] S. Feng, R. Chen, J. Lin et al., "Gastric cancer detection based on blood plasma surface-enhanced Raman spectroscopy excited by polarized laser light," *Biosensors and Bioelectronics*, vol. 26, no. 7, pp. 3167–3174, 2011.

[16] D. Graham, W. E. Smith, A. M. T. Linacre, C. H. Munro, N. D. Watson, and P. C. White, "Selective detection of deoxyribonucleic acid at ultralow concentrations by SERRS," *Analytical Chemistry*, vol. 69, no. 22, pp. 4703–4707, 1997.

[17] K. Faulds, R. P. Barbagallo, J. T. Keer, W. E. Smith, and D. Graham, "SERRS as a more sensitive technique for the detection of labelled oligonucleotides compared to fluorescence," *Analyst*, vol. 129, no. 7, pp. 567-568, 2004.

[18] M. Vendrell, K. K. Maiti, K. Dhaliwal, and Y.-T. Chang, "Surface enhanced Raman scattering in cancer detection and imaging," *Trends in Biotechnology*, vol. 31, no. 4, pp. 249–257, 2013.

[19] T. Troy, D. Jekic-McMullen, L. Sambucetti, and B. Rice, "Quantitative comparison of the sensitivity of detection of fluorescent and bioluminescent reporters in animal models," *Molecular Imaging*, vol. 3, no. 1, pp. 9–23, 2004.

[20] D. Graham and K. Faulds, "Quantitative SERRS for DNA sequence analysis," *Chemical Society Reviews*, vol. 37, no. 5, pp. 1042–1051, 2008.

[21] R. Duncan, "Polymer conjugates as anticancer nanomedicines," *Nature Reviews Cancer*, vol. 6, no. 9, pp. 688–701, 2006.

[22] J. R. Mccarthy, K. A. Kelly, E. Y. Sun, and R. Weissleder, "Targeted delivery of multifunctional magnetic nanoparticles," *Nanomedicine*, vol. 2, no. 2, pp. 153–167, 2007.

[23] M. C. Woodle and P. Y. Lu, "Nanoparticles deliver RNAi therapy," *Materials Today*, vol. 8, no. 8, pp. 34–41, 2005.

[24] Z. Medarova, W. Pham, C. Farrar, V. Petkova, and A. Moore, "In vivo imaging of siRNA delivery and silencing in tumors," *Nature Medicine*, vol. 13, no. 3, pp. 372–377, 2007.

[25] C. L. Zavaleta, B. R. Smith, I. Walton et al., "Multiplexed imaging of surface enhanced Raman scattering nanotags in living mice using noninvasive Raman spectroscopy," *Proceedings of the National Academy of Sciences*, vol. 106, pp. 13511–13516, 2009.

[26] M. Y. Sha, H. Xu, M. J. Natan, and R. Cromer, "Surface-enhanced Raman scattering Tags for rapid and homogeneous detection of circulating tumor cells in the presence of human whole blood," *Journal of the American Chemical Society*, vol. 130, no. 51, pp. 17214-17215, 2008.

[27] A. J. Frank, N. Cathcart, K. E. Maly, and V. Kitaev, "Synthesis of silver nanoprisms with variable size and investigation of their optical properties: a first-year undergraduate experiment exploring plasmonic nanoparticles," *Journal of Chemical Education*, vol. 87, no. 10, pp. 1098–1101, 2010.

[28] N. Leopold and B. Lendl, "A new method for preparation of highly surface-enhanced Raman scattering (SERS) active silver colloids at room temperature by reduction of silver nitrate with hydroxylamine hydrochloride," *Journal of Physical Chemistry B*, vol. 107, no. 24, pp. 5723–5727, 2003.

[29] J.-H. Kim, J-S. Kim, H. Choi et al., "Nanoparticle probes with Surface enhanced Raman spectroscopic tags for cellular cancer targeting," *Analytical Chemistry*, vol. 78, no. 19, pp. 6967–6973, 2006.

[30] S. Duraipandian, M. S. Bergholt, W. Zheng et al., "Real-time Raman spectroscopy for in vivo, online gastric cancer diagnosis during clinical endoscopic examination," *Journal of Biochemical Optics*, vol. 17, no. 8, article 081418, 2012.

[31] Y. Qin, X. Ji, J. Jing, H. Liu, H. Wu, and W. Yang, "Size control over spherical silver nanoparticles by ascorbic acid reduction," *Colloids and Surfaces A: Physicochemical and Engineering Aspects*, vol. 372, no. 1–3, pp. 172–176, 2010.

[32] X. Dong, X. Ji, H. Wu, L. Zhao, J. Li, and W. Yang, "Shape control of silver nanoparticles by stepwise citrate reduction," *Journal of Physical Chemistry C*, vol. 113, no. 16, pp. 6573–6576, 2009.

[33] J. S. González-Solís, G. H. Luévano-Colmenero, and J. Vargas-Mancilla, "Surface enhanced Raman spectroscopy in breast cancer cells," *Laser Therapy*, vol. 22, no. 1, pp. 37–42, 2013.

[34] L. Guerrini, N. Pazos-Perez, E. Garcia-Rico, and R. Alvarez-Puebla, "Cancer characterization and diagnosis with SERS-encoded particles," *Cancer Nanotechnology*, vol. 8, no. 1, 2017.

[35] H. Karabeber, R. Huang, P. Iacono et al., "Guiding brain tumor resection using surface-enhanced Raman scattering nanoparticles and a hand-held Raman scanner," *ACS Nano*, vol. 8, no. 10, pp. 9755–9766, 2014.

[36] Z. Movasaghi, S. Rehman, and J. U. Rehman, "Raman spectroscopy of biological tissues," *Applied Spectroscopy Reviews*, vol. 42, no. 5, pp. 493–541, 2007.

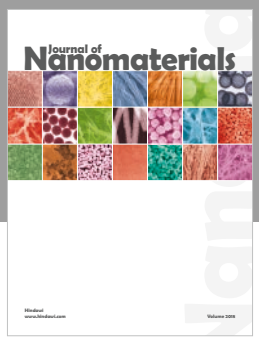

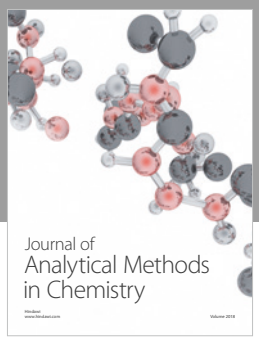

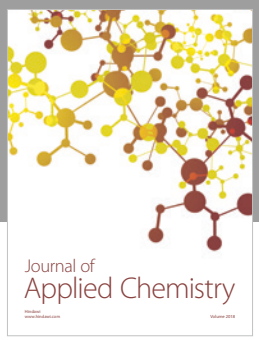

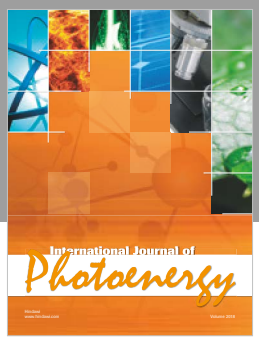

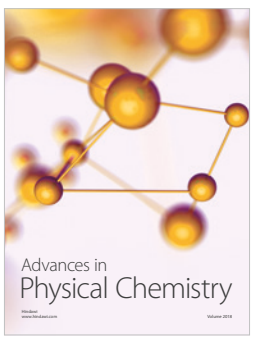

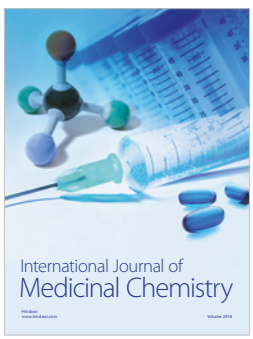

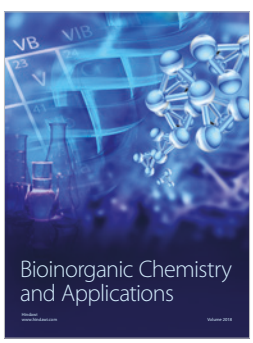

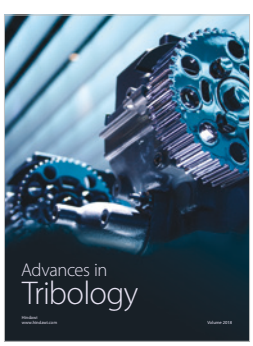

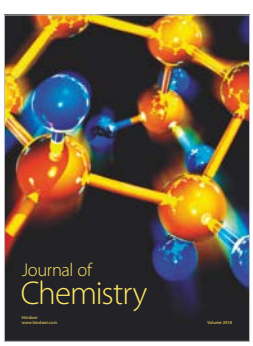

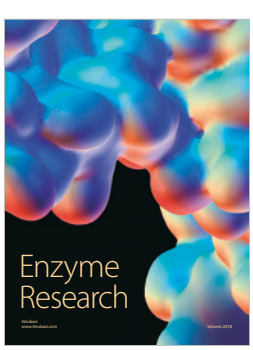

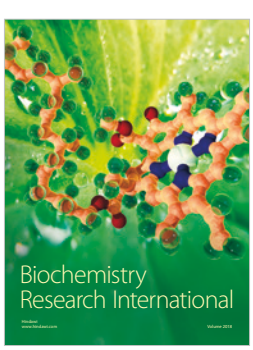

Hindawi

Submit your manuscripts at
www.hindawi.com